Z. Geomorph. N. F.	Suppl.-Bd. 35	60–80	Berlin · Stuttgart	August 1980

Experimental investigation of Horton overland flow on tropical hillslopes

2. Hydraulic characteristics and hillslope hydrographs

by

THOMAS DUNNE and WILLIAM E. DIETRICH, Seattle

with 7 figures and 1 photo

Zusammenfassung. Auf verschiedenen Berghängen Kenyas wurden auf 5 m langen Parzellen die Charakteristika des Abflusses während künstlich erzeugter Starkregen gemessen. Es zeigte sich eine unregelmäßige Schichtflut, aber es bildeten sich keine Rillen; generell waren die Hänge frei von Rillen.

Über der Parzelle wuchs die Gleichförmigkeit der Abflußmächtigkeit mit der Zunahme der Mächtigkeit des Abflusses und mit der Abnahme der Vegetation. Die Mächtigkeit veränderte sich mit der halben Potenz der Entfernung entlang der Parzelle und suggerierte, daß das Auftreffen von Regentropfen auf die Wasserschicht sowie die Wirbelbildung um Schotter und Vegetation ein Abflußverhalten zwischen laminar und turbulent erzeugten.

Jedoch kannn der Darcy-Weisbach Reibungsfaktor f als eine Funktion der Reynoldschen Zahl N_R aufgefaßt werden gemäß der laminaren Fließtheorie; d. h. $f = K/N_R$, wobei K als der Index für die Rauhheit von Mikrorelief und Vegetation dient. Der Übergang zum voll entwickelten turbulenten Fließen – wie er bei einem konstanten Reibungsfaktor zu erwarten wäre – konnte nicht beobachtet werden; er muß demnach erst bei einer Reynold-Zahl von über 1000 eintreten.

Um die hydrographischen Werte für die Berghänge Kenyas zu berechnen, wurde die HENDERSON-WOODINGsche kinematische Approximation modifiziert, um den Einfluß der Infiltration nach dem Ende der Starkregen mit zu erfassen. Unsere Berechnungen zeigen, daß nach dem Starkregen die Abflußdauer hangabwärts zunimmt. Nach Aufhören der Regen liefern lediglich die unteren Teile der meisten Hänge Abfluß zum Vorfluter, weil der meiste Regenwasser-Überschuß auf der Bodenoberfläche durch die Infiltration aufgezehrt wird, was eine räumliche Veränderung der Bodenfeuchte hervorruft.

Die Differenzen der hydrographischen Werte aus drei Gebieten Kenyas mit gleichen Niederschlags-Überschüssen wurden vorrangig durch die großen Unterschiede des Fließwiderstandes hervorgerufen, der sowohl die Zeit bis zum stabilen Abflußverhalten als auch die Dauer des Abflusses beeinflußt. Es sind deshalb sorgfältige Untersuchungen über den Abflußwiderstand auf den natürlichen Hangoberflächen notwendig.

0044-2798/80/0035-0060 $ 5.25

Summary. Characteristics of flow over a variety of Kenyan hillslopes were measured during artificial rainstorms on 5 m-long plots. An irregular sheetflow developed, but no rills formed, and in general the hillslopes were free of rilling. Uniformity of flow depth across the plot increased as the flow deepened and as vegetation cover declined. Depth varied as the 0.5 power of distance along the plot, suggesting that the bombardment of the flow by raindrops and the vortices generated around gravel and vegetation caused the flow regime to be intermediate between laminar and turbulent. However, the Darcy-Weisbach friction factor, f, could be expressed as a function of Reynolds number, N_R, according to laminar flow theory; i. e. $f = K/N_R$, and K served as an index of the roughness of microtopography and vegetation. Transition to fully developed turbulent flow, as would be suggested by a constant friction factor, was not observed and must occur at Reynolds numbergreater than 1000. In order to compute hydrographs for the Kenyan hillslopes the HENDERSON-WOODING kinematic approximation was modified to include the effects of infiltration after the end of the rainstorm. Our calculations show that the duration of runoff after the rainstorm increases downslope. Only the lower parts of most slopes contribute runoff to the channel after rainfall ceases because most of the excess precipitation remaining on the soil surface is consumed by infiltration, causing a spatial variation of soil-moisture recharge. In Kenya, differences between hillslope hydrographs from three regions for similar rates of pecipitation excess are caused primarily by large differences in flow resistance, which affect both the time to steady state runoff and the duration of runoff. Careful studies are therefore needed of the flow resistance on a variety of natural hillslope surfaces.

Résumé. Nous avons mesuré les caractéristiques d'écoulement sous pluie artificielle sur des parcelles de terrain longues de 5 mètres situées sur une variété de pentes au Kenya. Une nappe d'eau irrégulière s'est formée mais sans ruisselet, et dans l'ensemble aucun ruisselet ne s'est développé sur ces pentes. Nous avons observé un accroissement dans l'uniformité de la profondeur du plan d'eau avec l'approfondissement de la nappe et la diminution du couvert végétal. La profondeur varie proportionellement à la racine carrée de la longueur du plan, indiquant que le bombardement des gouttes de pluie sur la nappe, et les remous engendrés autour des pierres et des plantes provoquent un régime d'écoulement intermédiare entre laminaire et turbulent. Cependant le coefficient de résistance Darcy-Weisbach, f, peut être exprimé comme une fonction du chiffre de Reynolds, N_R, selon la théorie d'écoulement laminaire; c'est-à-dire $f = K/N_R$, K servant d'indice de rugosité de la microtopographie et du couvert végétal. Nous n'avons pas remarqué de transition à l'état turbulent pur dans l'écoulement, caractérisé par un coefficient de résistance constant, et la réalization de cet état semble indiquer un chiffre de Reynolds au dessus de 1000. Pour calculer quelques hydrographes de pentes au Kenya, nous avons utilisé la méthode cinématique de HENDERSON and WOODING, modifiée afin d'inclure les effets dus à l'infiltration après la pluie. Nos calculs montrent que la durée de l'écoulement après la pluie augmente en aval. En moyennes, seules les parties inférieures des pentes, après la pluie, contribuent à l'écoulement destiné pour la rivière. La majorité du surplus de précipitation résidente à la surface, étant absorbée, produit une variation spatiale dans l'humidité du sol. Dans trois régions au Kenya, les différences entre hydrographes pour des collines soumises à un régime similaire de précipitation excédentaire sont dues à de larges variations dans la rugosité hydraulique, qui retarde l'équilibre de l'écoulement et augmente la durée d'écoulement. Des études approfondies de la résistance hydraulique sur une variété de surfaces naturelles sont nécessaires.

Introduction

In a companion paper DUNNE & DIETRICH (this volume) have described the topographic and edaphic conditions that control infiltration and Horton overland flow on heavily grazed savanna hillslopes in Kajiado District, southern Kenya. In this paper we examine the hydraulic characteristics of the runoff, as measured

on 5 m-long plots under simulated rainfall. With the aid of these results we calculate runoff hydrographs from hypothetical planar hillslope segments in order to examine the effects of factors such as rainfall intensity, infiltration capacity, hillslope length and gradient, and vegetation density on runoff depth, velocity and discharge at various distances from the ridgetop. A later report will describe similar calculations for the case in which the first two of these controlling factors vary with time, and the last four vary along the hillslope profile. However, it is instructive to examine their effects individually first. The study area, plots, rainfall simulator, and sequence of experiments are described by DUNNE & DIETRICH (this volume).

Previous work

Most of the published information on the hydraulic characteristics of Horton overland flow pertains to artificial plots (e. g. PARSONS 1949; IZZARD 1944) or to wide, shallow channels (e. g. REE 1939). EMMETT (1970) has provided the most comprehensive set of hydraulic data for sheetflow over plots on natural hillsides, but the results were so variable that no consistent relationships emerged for these extremely rough surfaces. Important questions remain about the variation of flow resistance and the flow regime along a hillslope profile.

Each of the studies mentioned above involved direct measurement of mean flow depth and velocity and the calculation of resistance coefficients. In several other investigations these hydraulic characteristics have been back-calculated from plot or basin hydrographs without measurement of the spatial variation of the flow (e. g. MORGALI 1970; WOOLHISER et al. 1970; LANGFORD & TURNER 1972). The back-calculation methods are attractive because they reduce the necessary field measurements, and because they avoid the difficulty of measuring the depth of flow over irregular natural hillslopes. On many hillsides, the assumption of a relatively uniform sheet of Horton overland flow is untenable because the runoff is concentrated into rills and gullies. However, it is still possible to compute "equivalent" depth and resistance parameters for the runoff and to use them to predict the response of runoff in other storms. SINGH (1976) has proposed that in such cases, the complex form of natural hillsides be represented by a simple converging surface fitted to the entire catchment.

However, there is a need for direct measurements of runoff hydraulics on natural hillslopes in order to characterize the actual values of depth, velocity, resistance, their local variability and systematic variation along hillslopes. The spatial variability is particularly important in geomorphology because it is hoped that eventually it will be possible to progress from a sound theory of runoff to a theory of hillslope erosion and evolution that is based upon the spatial pattern of hydraulic characteristics, shear stress, and sediment transport. In pursuit of such a goal we have made a limited investigation of runoff properties on hillslopes that are remarkably smooth, and for which the sheetflow approximation appears to be acceptable. As will be described later, there was some variation in flow-depth along the contour during the experiments, but no tendency for rill or gully development exists on the upper few hundred metres of the hillslopes. The investigation of runoff and sediment transport on rilled slopes is likely to be

much more complicated, however, and will require the development of an efficient quantitative method of describing the degree of flow convergence (FOSTER & MEYER 1975).

Experimental method

We subjected 5 m-long plots to one-hour rainstorms of various intensities that produced runoff rates of 20–164 mm/hr (DUNNE & DIETRICH, this volume, tables 1 and 2). In almost all experiments infiltration and runoff attained constant rates and most of the hydraulic measurements were conducted under those circumstances. Some measurements were made on the rising limb of the hydrograph, but the methods were not sufficiently precise to reflect such an effect. Measurements were made on the relatively thickly-vegetated clay Vertisols of plots 3 and 5 on the Athi-Kapiti Plains, the sparsely vegetated sandy clay Luvisols of plots 6, 7, 10, and 11 on the Amboseli Basement, and the unvegetated sandy clay Luvisols covered with various amounts of surface gravel on plots 12, 13, and 14 on the Kilimanjaro Lava at Kimana. The gradients, vegetation covers, rainfall intensities and discharges for each plot during each experiment are listed in the companion paper. Photo 1 shows representative plot surfaces.

Hydraulic data were collected by two rather crude methods. First, the depth of overland flow was measured to within 1 mm with a thin scale at five equally-spaced points across the plot at distances of 0.1 m or 0.2 m, 1 m, 2 m, 3 m, and 4 m from the upper boundary. The average depth and the steady-state discharge at each distance (calculated as a proportion of the measured discharge at the base of the plot) were used to compute the mean velocity. The second method involved measurements in local threads of flow. Average depth was measured with the scale at five points along an obvious flow path between 0.5 m and 1.0 m long. A small slug of dye was then injected into the flow. Very little of the dye diffused through the water and almost all of it travelled as a dense cloud. The velocity of the leading edge of the slug was measured over the 0.5 m- or 1.0 m-long path and was taken to represent the surface velocity, which when multiplied by 0.67 yielded the vertically averaged velocity for laminar flow (HORTON et al. 1934). It was not possible to separate depression storage from detention storage in the depth measurement.

There was a tendency for the flow depth to be over-estimated by about 0.5 mm because the scale sank slightly into the wet soil. The mean depth across a contour was probably not in error by more than half of this amount. Exaggeration of the depth had the effect of reducing the computed mean velocity in the first method, and of increasing the Darcy-Weisbach resistance parameter (see later). Over most of the plots this measurement error could cause the depth to be over-estimated by about 5 percent, although at the upper ends of a few plots, particularly on the smooth slopes, errors of 30 percent or more were possible. The smaller error could increase the computed resistance factor by 16 percent, and the larger error could exaggerate the resistance parameter by more than twofold. Fortunately, the sandy clay plots which had the shallowest flows at their upper ends also had the firmest sandy surfaces, and because the scale was placed with great care the errors probably did not approach the upper limit

discussed here. The agreement between our results and those of others supports this claim.

Flows along the paths measured by the second method were deeper than the average flow, so that the potential exaggeration of the depth was almost always less than 10 percent. Such an error had only a linear effect on the computed Darcy-Weisbach resistance coefficient because the velocity was measured independently. The velocity was probably overestimated by a small amount because the velocity of the centre of mass of the dye should have been recorded instead of that of the leading edge. In the absence of a colorimeter, we had to use the latter index. Some spreading of the dye cloud occurred, so that the centre of mass travelled more slowly than the leading edge. However, very little of the dye composed the trailing limb of the slug, and travel time of the centre of mass could not have exceeded that of the leading edge by more than ten percent. Such an overestimation of the velocity would generate an exaggeration of up to 10 percent in the Reynolds Number and a maximum reduction of 21 percent in the friction factor. Such errors would partly offset one another in the definition of the inverse relationship between Reynolds Number and friction factor (see later).

The crudeness of the measurement techniques obviously limits the reliability of the results, but the latter are in general agreement with the few other comparable sets of data, indicating that despite the simplicity required by the field conditions the hydraulic relations were approximately defined over a range of natural conditions.

Character of sheetflow

The nature of the sheetwash varied between plots because of the differences in ground cover, but displayed no tendency for the incision of rills. On the Athi-Kapiti Plains the relatively dense vegetation and associated microtopography of plots 3 and 5 (poto 1 a, b) confined most of the runoff into meandering and anastomosing paths amid a generally shallower and slower sheet which covered the whole plot. EMMETT (1970: A 1) described the same phenomenon on rangelands in Wyoming. On the Amboseli plots (photo 1 c) with a much thinner vegetation cover, the same pattern of flow concentration occurred but local differences in depth and velocity were less extreme. The Kilimanjaro plots had smoother surfaces without vegetation cover (photo 1 d, e) although 92 percent of plot 12 was covered with gravel (D_{50} = 11 mm), approximately 5 percent of plot 14 was covered with gravel up to 30 mm in size, and plot 13 had a sprinkling of 4–8 mm gravel which covered about 1–2 percent of the surface. Variations of depth and velocity occurred on the Kilimanjaro plots, but flow was not disrupted to the extent observed on the plots with a vegetation cover.

As a measure of the depth variability across each plot we computed the coefficient of variation of the five measurements at each distance from the upper

Photo 1. Surface conditions on plots: (a) Representative of plots 3 and 5 on Athi-Kapiti Plains before clipping, average ground cover 77 %; (b) Athi-Kapiti plots after clipping to basal cover, average ground cover 36 %; (c) Plot 10 at Amboseli, average ground cover 12 %; (d) Gravel-covered surface of plot 12, Kimana; (e) Bare plot 13, Kimana.

Photo 1 a

Photo 1 b

Photo 1 c

Photo 1 e

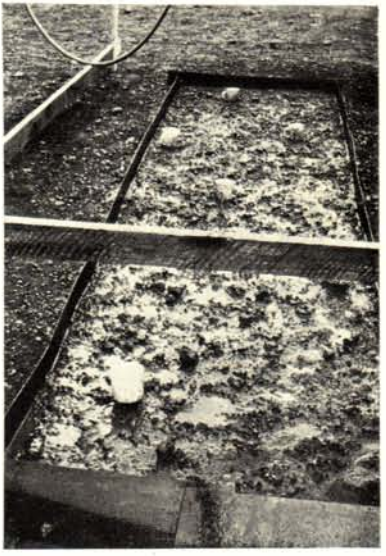

Photo 1 d

boundary. The coefficient (which was defined poorly from only five measurements) generally bore an inverse relationship to the mean flow depth as the latter varied along the plot and with runoff rate (fig. 1). On the bare, relatively smooth plot 13, for example, the coefficient of variation indicated that two-thirds of all depth measurements should lie within 20 percent of a mean depth of 4 mm, and this value increased to 60 percent of the mean depth of a flow 1 mm deep. The inverse relationship reflected both the measurement errors discussed above and

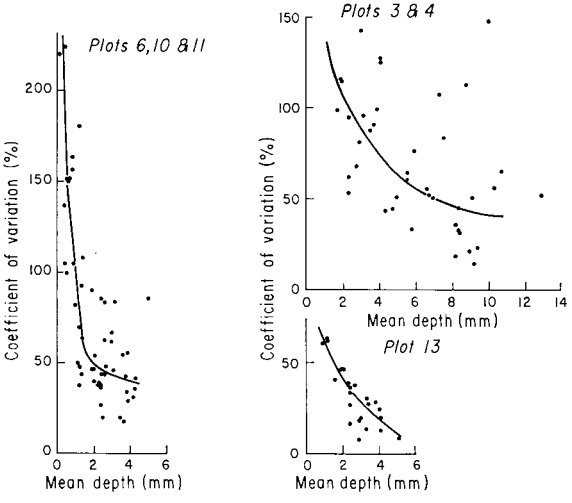

Fig. 1. Coefficient of variation of depth plotted against mean depth of sheetflow based on five measurements along a contour. Plots 6, 10 and 11 are at Amboseli, plots 3 and 5 on the Athi-Kapiti Plains, and plot 13 is at Kimana. The curves join the approximate median values of the coefficient of variation in each depth class.

the fact that in the shallowest flows even the smallest surface protuberances can divide the flow to an important degree. On the rougher Amboseli plots, with ground covers that ranged from 8 to 41 percent, the average coefficient of variation declined from over 100 percent at a 1 mm depth to about 40 percent at 4 mm. On vegetated plots 3 and 5 on the Athi-Kapiti Plains profiles of depth were measured only during the "clipped" and "intense" runs (see DUNNE & DIETRICH, this volume) when the ground cover had been reduced to 36 percent. The flow depths were greater than on the sandy clay plots, and were so variable that it is even difficult to generalize about the coefficient of variation. At flow depths between 8 and 13 mm, the coefficient usually ranged from 15 to 60 percent and increased to 50–150 percent at flow depths of 2–4 mm. The local variation in flow depth was greatly increased by the presence of vegetation and gilgai microtopography.

As mentioned above, this variability in depth means that the concept of a uniform sheetflow is an abstraction. Furthermore, the meandering and anastomosing patterns of flow and the variation in velocity as water spills over a clump of grass or flows around an obstruction render suspicious the assumption of steady, uniform flow made in all resistance laws used for runoff computations. Until there is developed a measurement technique and computational scheme able to take account of these local and temporal variations of momentum, the sheet-

flow approximation will be necessary. It is still a matter of judgment whether the approximation is adequate on a particular hillslope.

Average flow depths varied along each plot, as shown in the examples in fig. 2, increasing with runoff rate (fig. 2 a) and with surface roughness (comparison between fig. 2 b and the upper curve in fig. 2 a for which the runoff rates were equal). Regression analysis indicated that on most plots both mean depth and mean velocity increased with the 0.5 power of distance from the upper plot boundary. This relationship suggests that the flow regime is intermediate between laminar, for which the exponent on depth should be 0.33, and turbulent, for which it should be 0.67.

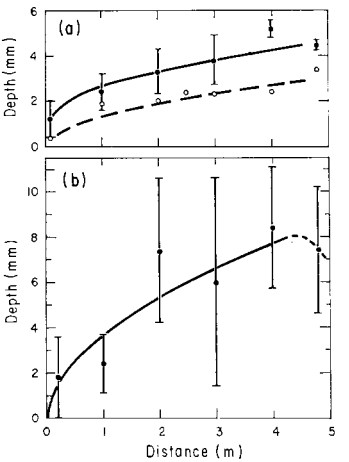

Fig. 2. Steady-state profiles of sheetflow depth on plots. The points represent the mean of five measurements made along a contour, and the bars indicate the standard deviation of the measurements. (a) Plot 13, solid curve, runoff rate = 85 mm/hr; dashed curve, runoff = 27 mm/hr. (b) Plot 3, Athi-Kapiti Plains, runoff rate = 85 mm/hr. Some of the masurements at a distance of 4.8 m indicate drawdown near the runoff collector, and were not used for calculation of the hydraulic parameters in this paper.

The injected dye tended to move in smooth trajectories until it was disturbed by raindrops and by wakes behind grass stems and clumps. Turbulence imposed by these two mechanisms was damped, and there were only local tendencies for the spontaneous generation of vortex instabilities near the boundary as indicated by trajectories of sediment and small organic particles in zones that were not receiving raindrops at the time. EMMETT (1970) called such a flow regime "disturbed laminar flow," and HORTON (1945) referred to runoff through vegetation stems as "subdivided flow."

Flow resistance

The resistance formulae commonly used in hydraulics for steady flow in pipes and channels were not derived to deal with some of the characteristics of overland flow, such as the local accelerations and changes in depth referred to previously, the presence of an eroding boundary, important effects of raindrop impacts, and form roughness effects due to the occurrence of relatively large elements such as plant stems, gravel, and microtopography which may protrude from the free surface. However, an assumption is usually made that the Darcy-Weisbach resistance formula is appropriate for the description of overland flow,

and we found that on the Kenyan hillsides it yielded results of a general form that is predicted by theory. We have used the following form of the Darcy-Weisbach equation

$$(1) \qquad \bar{u}^2 = \frac{2\,ghs}{f}$$

where $\bar{u}$ is the vertically averaged mean flow velocity, g is the gravitational acceleration, h is the mean flow depth (all in mks units), s is the gradient of the water surface, and f is the dimensionless friction factor. Although the measured depth profiles allowed the calculation of water surface gradients, we judged that such a correction would lead to an illusory improvement in the light of the earlier discussion of depth and velocity variation. Therefore, we have used the average plot gradient for s in the equation; the maximum error from this approximation is 5–10 percent. We have used the constant 2 in equation (1) to conform with the theoretical derivation given by STREETER & WYLIE (1975: 287), rather than the pipe-flow form with a constant 8 that is commonly used for overland flow. Previously published values of the friction factor should be divided by 4 for comparison with our values.

Values of the Darcy-Weisbach friction factor were calculated by inserting the field measurements into equation (1), and they were plotted in the conventional form of a Moody diagram (fig. 3) against the local flow Reynolds Number ($N_R = \bar{u}h/\nu$ or $N_R = q/\nu$, where q is the discharge per unit width of hillside and ν is the kinematic viscosity of water at the ambient temperature). The results indicated large differences between flow resistance on the various surfaces, and on each type of surface f generally declined as N_R increased in the laminar range. This inverse relationship between f and N_R has been documented for laminar flow over many surfaces, and theory predicts that the relationship should be linear (HORTON et al. 1934; STREETER & WYLIE 1975). Least-square regression lines through our data were steeper than predicted by theory, but we ascribe this discrepancy mainly to the previously-mentioned overestimate of depth and therefore friction factor in the shallow flows at the upper ends of the plots. We have therefore constrained the slope of the regression lines through each data set to have a slope of — 1.0, producing the equations of the conventional form

$$(2) \qquad f = \frac{K}{N_R}$$

where K is a dimensionless parameter describing the roughness of each hillslope surface.

There is a large amount of scatter around each line because of measurement errors, real local differences over the plot, and differences between plots. EMMETT (1970), whose technique of depth measurement was more precise than ours, found essentially the same degree of local variation in resistance as the flow was diverted and channelled by vegetation and gravel, or as it spilled from one shallow depression to another. In spite of the variability, the inverse relationship between f and N_R is well-defined for each surface with the possible exception of the Amboseli sites where a local f-value can vary by more than an order of magnitude for a fixed Reynolds Number.

The K-values reflect the different surface morphologies of the plots. The few

square symbols in fig. 3 a, which are from unclipped vegetation on plots 3 and 5 (with an average ground cover of 77 %), define a line with K = 13,250, which is

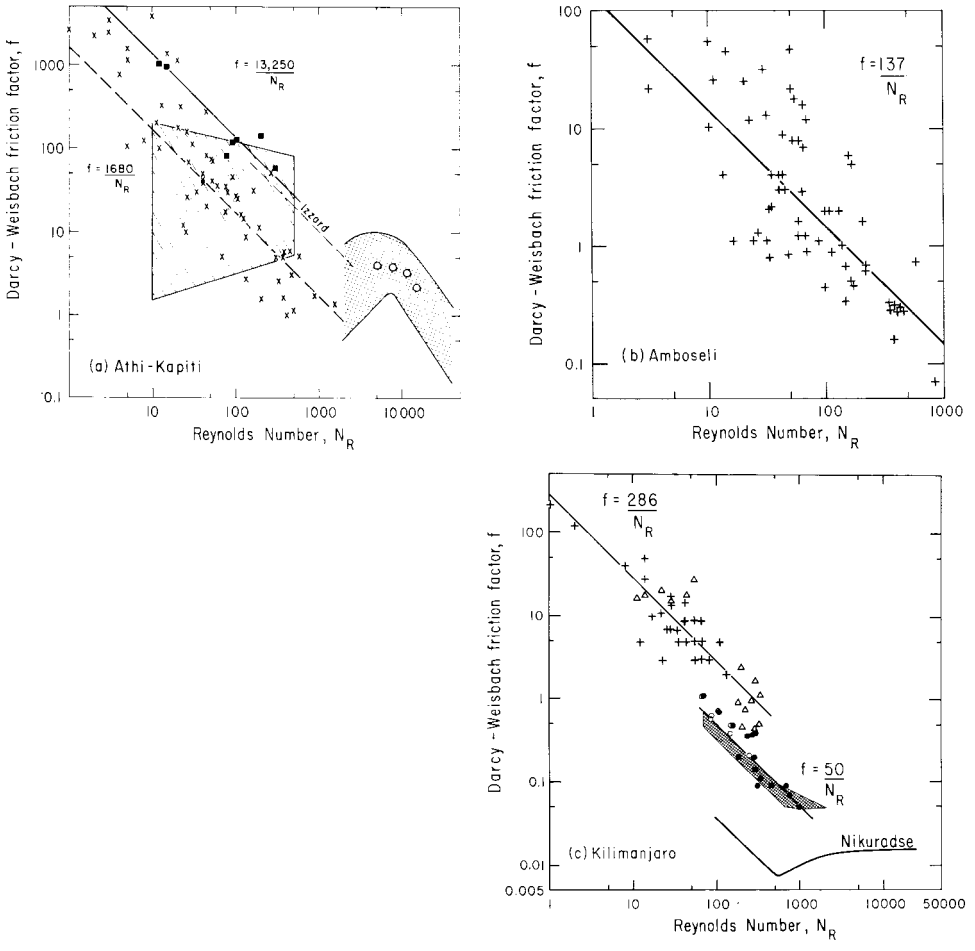

Fig. 3. Moody diagram for various surfaces. (a) Solid squares and line are from original cover of 77 % on plots 3 and 5, Athi-Kapiti Plains. Crosses and dashed line are from clipped basal cover of 36 % on same surfaces. Lined area is the region of EMMETT's (1970) measurements on natural hillsides with a cover of 8–35 %; cross-hatched area indicates the extent of measurements by KAO and BARFIELD (1978) on flow over artificial grass in a flume; the open circles are from a grass-covered flume studied by REE (1939), and the short dashed line summarizes IZZARD's (1944) data from turf. (b) Plots 6, 10 and 11 at Amboseli with ground cover varying between 10 and 41 %. (c) Triangles are from plot 12 and crosses from plot 13 on the Kilimanjaro lavas at Kimana. Solid circles are from measurements in threads of concentrated flow in sandy zones of plot 13. Open circles are from measurements over an immobile sandy surface by LANGFORD & TURNER (1972). Data from SIMONS & SENTÜRK (shaded area) are for laboratory sand channels and those of NIKURADSE are for flow over sand glued to the insides of pipes.

close to IZZARD's (1944, fig. 4 b) relationship for turf on smooth plots, and which leads into the region of data for shallow turbulent flows in grassed channels (REE 1939; KAO & BARFIELD 1978). The same plots with the cover clipped to an average of 36 % yielded a K value almost an order of magnitude lower. The data from these grassy plots on the Athi-Kapiti Plains fall into the same general region as the measurements of EMMETT (1970) for rough Wyoming hillsides with ground covers of 8–31 percent.

At Amboseli (fig. 3 b), under vegetation covers of 10, 16, and 41 percent the friction factor averages another order of magnitude below that for the clipped run on the Athi-Kapiti Plains. The data from a 41 percent cover at Amboseli (plot 11) lie close to those for the 10- to 16-percent basal covers rather than to the measurements under a 36-percent cover on the Athi-Kapiti Plains. On the Amboseli plots, the vegetation was clumped so that the water flowed in smoother trajectories around clumps and the associated microtopography. On the Athi-Kapiti Plains, the basal cover was more dispersed, the microtopography was rougher (fig. 2), and they disrupted the flow more severely. This suggests that measurement of vegetation density alone may not be an adequate index of hydraulic roughness unless the microtopography induced by vegetation is directly related to cover density.

On the bare Kilimanjaro plot 13, the friction factors, computed from average depths and calculated velocities, were slightly larger than those from Amboseli (fig. 3 c). The sparse cover of gravel particles (photo 1 e) generated drag forces and wakes which raised the friction factor. Surprisingly, the coarse, almost complete, gravel cover on plot 12 (photo 1 d) yielded similar friction factors to those on plot 13. WOOLHISER (1975) also reported that K-values for a gravel surface were virtually identical to those from an eroded, bare clay loam, although his range of values calculated from hydrographs were significantly lower than those reported here. By comparison, dye measurements in the deeper and faster streams on sandy zones relatively free of gravel on plot 13 indicated friction factors that define a lower line. These lower friction factors agree closely with two other sets of data shown in fig. 3 c. Seven measurements by LANGFORD & TURNER (1972) under artificial rainfall on a sand surface stabilized by bitumen (open circles in fig. 3 c) agree almost exactly with the average line through the Kilimanjaro points for the sandy zones. Also, friction factors for small, sand-bedded laboratory channels (SIMONS & SENTURK 1978: 308) plot slightly below those of the sand-bedded threads of flow on plot 13. Finally, the results of experiments conducted by NIKURADSE (reported by STREETER & WYLIE 1975: 296) on flow through pipes roughened with immobile sand plot below the values for the field sites with more complicated microtopography.

Raindrop impacts may have a significant influence on the hydraulics of overland flow. First, the raindrops which enter the sheetflow with no horizontal momentum must be accelerated up to the mean flow velocity. This rate of withdrawal of momentum per unit area of the fluid imposes a shear stress, τ_r, which is equal to the product of fluid density, rainfall intensity, and mean sheetflow velocity. The maximum value of τ_r during our experiments was 0.009 Nt/m^2, two to three orders of magnitude less than the total boundary shear stress at the lower ends of the plots. Turbulence generated by the raindrop impact causes

energy loss and increased flow resistance, which is particularly important in laminar films over smooth surfaces (YOON & WENZEL 1971). As the flow becomes more turbulent or as the resistance increases due to a vegetation cover, the raindrop effect becomes insignificant (IZZARD 1944). In the absence of a good theoretically-based computation of the effects of raindrops on flow resistance, WOOLHISER (1975) summarized empirical equations describing the effect of rainfall intensity on K-values calculated from hydrograph analysis. The empirical relations indicate negligible effects on rainfall intensity on the vegetated Kenyan plots, but yield negative values of corrected friction factor on the bare plot. Furthermore, LANGFORD & TURNER (1972) have suggested that if well-developed separation zones are created in laminar flow by flow past protruding particles of sand or small mounds, turbulence induced by raindrop impact may dampen the tendency for flow to separate and thus may reduce flow resistance. Further experimentation is needed to resolve this uncertainty and until there is clearer evidence for the role of raindrop impact, we report our uncorrected field data.

Although the inverse linear relationships of fig. 3 are predicted from the theory of laminar flow, the upper Reynolds Number at which laminar flow is stable can only be determined empirically. IZZARD (1944) demonstrated that the inverse relationship persists to Reynolds Numbers of 1000, while others, who calculated flow resistance from hydrographs, have suggested that the resulting Moody diagram demonstrates a transition to turbulent flow at Reynolds Numbers between 100 and 500 (MORGALI 1970; WOOLHISER et al. 1970; LANGFORD & TURNER 1972). Hot-film probe measurements by YOON & WENZEL (1971) in shallow flows under rainfall revealed that the flow contained eddies even in the conventional laminar range of N_R, while the friction factor behaved as predicted by laminar-flow theory up to $N_R = 2000$. Such a result confirms our field observations that the flow was constantly disturbed by raindrops and wakes, but that on the bare and sparsely vegetated plots the shallow depth inhibited the formation of vortices so that the imposed turbulence was damped and the resistance behaved dominantly as for a laminar fluid. Although the flow was deeper on the densely vegetated plots (3 and 5) the resistance also decreased up to Reynolds Numbers near 1000. It is possible that this laminar behaviour results because the movement of flexible grass stems removes from the fluid momentum that would otherwise be converted to eddies. The intermediate nature of the flow regime is suggested, however, by the downslope variation of discharge with the square of mean depth, as mentioned earlier.

For the purpose of computing hillslope hydrographs in this paper, we will use a laminar flow law for $N_R < 1000$. For comparison with overland flow under natural conditions, a Reynolds Number ($N_R = q/\nu$) of 1000 is produced by a runoff rate of 10 mm/hr within 360 m of the ridgetop and by 1 mm/hr within 3600 m at a water temperature of 20 °C. A later paper will consider the transition to turbulent flow. Although our field measurements extend only up to the transitional zone, theory and most experimental data indicate that the friction factor approaches a constant value in the turbulent regime (see STREETER & WYLIE 1975: 297). The behavior of the friction factor in the transitional and turbulent regimes of flow through grass is complex and not well understood (PHELPS 1970; KAO & BARFIELD 1978).

Hillslope hydrographs

The significance of the hydraulic properties of sheetflow can be illustrated by using them to compute runoff hydrographs from idealized planar hillslopes, which are reasonable approximations to long, gentle, savanna hillsides. Our calculations are based on the kinematic approximation pioneered by HENDERSON & WOODING (1964) and developed further by WOOLHISER (1975) and others. Because an alteration of the usual method was necessary to conform with field conditions, a brief outline of the procedure must be given here, but the reader is referred to the papers listed above for the mathematical derivations.

For overland flow on a plane it is first necessary to define the relation

$$q = \alpha h^m \tag{3}$$

where q and h are discharge per unit width and depth, m varies between 1.67 for fully turbulent flow and 3.0 for laminar flow, and α contains the gradient and roughness of the surface. For laminar flow, combination of eqs. (1) and (2) leads to $\alpha = 2\ gs/K\nu$. Taking the derivative of eq. (3) with respect to h and using the chain rule, one can re-write the continuity equation for one-dimensional overland flows as

$$\frac{\partial h}{\partial t} + \frac{\partial q}{\partial x} = \frac{\partial h}{\partial t} + \alpha m h^{m-1} \frac{\partial h}{\partial x} = p(x, t) \tag{4}$$

where p is the rate of precipitation excess (i. e. rainfall intensity minus infiltration capacity), x is distance downslope from the ridgetop, and t is time since the beginning of runoff.

Here we deal only with the case where p is constant in time and space. The former assumption is acceptable for a constant rainfall because when the Kenyan soils become wet, they attain a constant infiltration capacity within a few minutes of the onset of rainfall (DUNNE & DIETRICH 1980). Spatial uniformity of infiltration capacity restricts application of the results to hypothetical situations on hillslope segments, because infiltration capacity can vary systematically along slope profiles, as described in the companion paper. Such differences will be taken into account in a later paper. For the present purpose there is value in examining hydrographs from planar segments in order to study the effects of major controlling variables on hillslope runoff.

HENDERSON & WOODING (1964) demonstrated that equation (4) can be simplified by introducing the velocity

$$\frac{dx}{dt} = \alpha m h^{m-1} \tag{5}$$

which makes equation (4) take the form of the total derivative of h

$$\frac{dh}{dt} = p. \tag{6}$$

Because $h = 0$ at $t =$ integration of (6) yields

$$h = pt. \tag{7}$$

The introduced velocity, in this case, can be viewed as the speed at which an observer must travel along the hillslope in order to observe the results predicted by equation (6). The required movement downslope of the observer can be plot-

ted as a line on the x-t plane and that line is called a characteristic. An expression which predicts the characteristic for any starting point on the hillslope, x_o, at $t = 0$ is found by substituting equation (7) into (5) and integrating that latter to give

(8) $\quad x = x_o + \alpha p^{m-1} t^m.$

Fig. 4 shows the characteristics given by this expression for different starting points along the hillslope.

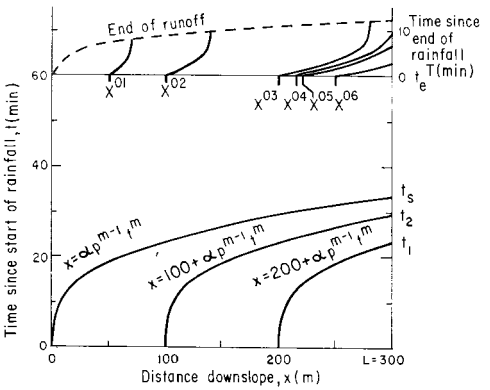

Fig. 4. Characteristics for the calculation of laminar runoff along a 300 m-long hillslope $\nu = 10^{-6}$ m²/s, p = 10 mm/hr.

Each characteristic that begins at some x_o reaches a channel at the base of the slope ($x = L$) at a time t, and along that characteristic and at the base of the slope before steady state is achieved the discharge of water is given by equation (9) which is obtained by substituting equation (7) into (3):

(9) $\quad q = \alpha p^m t^m$

Thus, characteristics from progressively higher on the slope reach the channel at progressively later times and the discharge at the base of the slope increases as a power function of time, defining the rising limb of the hydrograph (figs. 4 and 5).

Examining a characteristic that begins at the ridgetop ($x_o = 0$) at $t = 0$, one finds (fig. 4) that it reaches the base of the slope, $x = L$, at t_s where

(8 a) $\quad x = L = \alpha p^{m-1} t_s^m.$

The time, t_s, is the interval required for the whole slope to shed water to a channel at its base. At this time, according to equation (9)

(9 a) $\quad q_s = \alpha p^m t_s^m = pL,$

the peak rate of runoff, which is maintained until the end of rainfall (fig. 5). If the duration of the rainstorm is less than t_s the peak rate of runoff is given by equation (9) at the end of rainfall, t_e.

Because there are no effects on the runoff which propagate upslope in this formulation of the problem, eq. (8 a) can also be used to predict the time to steady state depth anywhere along the slope, not just at the foot, and the equation indicates that this time, t_s, increases as a power function of distance from the ridge. Thus, the maximum attainable depth, h_s, for any point on a hillslope

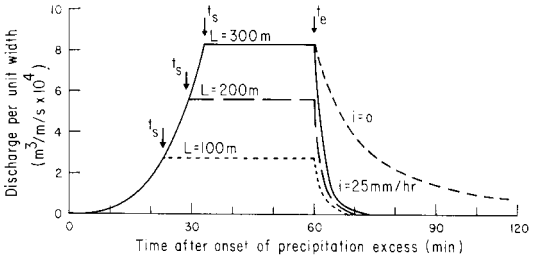

Fig. 5. Solid curve represents the hydrograph of runoff from a 300 m-long hillside with the properties specified in fig. 4. The curve labeled i = 0 indicates the form of the recession limb from the slope if there were no infiltration after the cessation of rainfall. Other dashed curves represent hydrographs from shorter portions of the hillslope.

profile develops first at the top of the hill and then spreads downslope. This depth is obtained by substituting (8) for $x_o = 0$ into (7):

$$h_s = \left(\frac{xp}{\alpha}\right)^{1/m} \tag{10}$$

Until the maximum depth is obtained at a point, the sheetflow thickness there is given by eq. (7). The distance from the ridge, x′, above which the depth has achieved steady state, is specified by

$$x' = \alpha p^{m-1} t^m \tag{11}$$

Upslope of x′, eq. (10) describes the depth profile, and downslope it is given by eq. (7). The along-slope variation of depth is created by the downslope translation of x′.

In order to compute the recession limb of the hydrograph, it is usual to assume that p = 0 at the end of rainfall which implies that the infiltration capacity is also zero, and to make the recession limb simply equal to the rate of drainage of the water in detention storage. This assumption that the infiltration capacity is zero is unacceptable on long, gently sloping hillsides with significant vegetation cover because it leads to the prediction that runoff continues for many hours after rainfall on the Kenya savanna. This prediction is not confirmed by our field experience because the detention storage after rainfall is mainly consumed by infiltration. We have therefore modified the kinematic-wave calculation procedure (of WOOLHISER 1975: 494–497, for example) to allow for infiltration after the end of a rainstorm. SHERMAN & SINGH (1976) have also considered the effect of infiltration on the hydrograph from a converging surface. Here we deal with the one-dimensional case.

The initial condition for the recession of the hillslope hydrograph is one of the profiles in fig. 6. A characteristic originating at some point on the hillside will

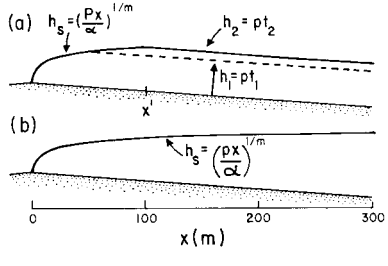

Fig. 6. Depth profiles of overland flow. (a) At t_2 the profile is indicated by the solid curve with the steady-state depth attained only above x′, below which the thickness grows linearly with time. (b) Steady state conditions extend over the whole hillside.

have the following governing equations, analogous to (5) and (6) for the rising limb:

(12) $$\frac{dh}{dT} = -i$$

(13) $$\frac{dx}{dT} = \alpha\, m h^{m-1}$$

where i is the infiltration capacity, and T is time since the end of rainfall (i. e. $t-t_e$). Integration of (12) yields

(14) $$h = h_0 - iT$$

where h_0 is the initial depth at the origin of the characteristic at T = 0, and is given (see fig. 6) by

(10 a) $$h_0 = \left(\frac{xp}{\alpha}\right)^{1/m} \text{ for } x \leqq x' \quad \text{and}$$

(7 a) $$h_0 = pt_e \text{ for } x \geqq x'$$

The distance downslope, x', is determined using eq. (11). Equation (14) can be inserted into (13) before the latter is integrated to give

$$x = -\frac{\alpha}{i}(h_0 - iT)^m + C$$

At T = 0, let $x = x^o$, the starting point of a trajectory in the x-T plane (see fig. 4). From these values

$$C = x^o + \frac{\alpha\, h_0^m}{i} \quad \text{and}$$

(15) $$x = x^o + \frac{\alpha\, h_0^m}{i} - (h_0 - iT)^m \frac{\alpha}{i}$$

Also analogous to the rising limb and steady state conditions, if an observer starts at some position on the slope, x°, where the water depth is h_0 at the end of rainfall, and moves downslope at the velocity specified by eq. (13), he will find the sheetflow thinning according to eq. (12), and in response his own velocity will decrease. After a sufficiently long time, the infiltration will have consumed the entire thickness of that element of the sheetflow, the term in parentheses in equation (15) will become zero, and that element of the sheetflow originating at x^o at the end of rainfall will have been absorbed by the soil (see fig. 4).

The procedure for calculating the recession limb of the hydrograph is as follows. A few x^o values (x^{01}, x^{02}, in fig. 4) are chosen along the line T = 0, and the sheetflow thickness, h_0, is computed for each point from the initial conditions specified in eqs. (7 a) and (10 a). For the case illustrated in figs. 4 and 5, the whole hillside has attained equilibrium (i. e. x' = L), and h_0 is specified everywhere by eq. (10 a). In order to compute the position of the characteristic at later values of T, h_0 is substituted into equation (15) which is solved for x at chosen values of T.

In the example shown in fig. 4, an element of sheetflow leaving $x^{02} = 100$ m travels only 40 m downslope at a decreasing rate before it is consumed and runoff ceases at that distance approximately 9 minutes after the end of the rainfall.

The thicker sheetflow element originating at $x^{03} = 200$ m is eventually consumed at 280 m. Characteristics from the lower few tens of metres of the slope reach the channel before all of the sheetflow is consumed, and so this part of the hillside contributes to the recession limb of the hydrograph. The discharges on the recession limb are obtained by inserting the time (T) at which a characteristic reaches $x = 300$ m into eq. (14) to obtain h, which is substituted into eq. (3). In the example shown in fig. 4, the infiltration capacity is 25 mm/hr, so that the sheetflow which is initially several millimetres thick is rapidly consumed, and the discharge declines rapidly, being supplied only by a narrow zone at the base of the slope. For comparison, fig. 5 also contains a recession limb computed on the basis of the common assumption that no infiltration occurs after rainfall. Even for the smooth hillside ($K = 100$), the recession limb is much longer than one observes in the field. Hydrographs from slopes of 100 m and 200 m are also shown in fig. 5.

Another useful product of a method that takes account of infiltration is the computation of the duration of runoff and infiltration at any distance along the hillside. The upper dashed curve in fig. 4 is a free boundary which indicates how the upper edge of the zone experiencing overland flow moves downslope after the rainstorm. One hundred metres from the ridgetop, runoff ceases at $T = 8.5$ min, whereas it continues until $T = 11$ min at the base of the slope. If the infiltration rate is constant through time, the total absorption is greater by 1 mm at the lower position. In this particular example, the effect is trivial and within computation errors, but repetition during the approximately ten runoff events of each year must have a slight effect on the spatial pattern of soil moisture and plant production.

Comparison of the recession limbs for $i = 0$ and $i = 25$ mm/hr in fig. 5 indicates another important effect on the soil-water balance of infiltration after rainfall on a 300 m-long hillside. A precipitation excess of 10 mm/hr for one hour does not yield 10 mm of runoff to the channel. By the end of the rainstorm (t_e), runoff totals only 6.2 mm. The remainder drains off slowly if the soil is impervious, but with an infiltration capacity of 25 mm/hr, a value typical of the sandy clay Luvisols during the wet season (DUNNE & DIETRICH this volume), less than 0.8 mm more leaves the hillside for a total runoff of only 7 mm. This discrepancy is enhanced on longer, gentler hillsides and on those with higher infiltration capacity and greater flow resistance, as well as during shorter rainstorms.

Controls of hydrograph form

Figure 7 includes hydrographs which reflect the influence of the range of hydrologic, hydraulic, and morphologic variables on the Kenyan hillsides. For example, a comparison of fig. 5 with figs. 7 a and 7 b for the same hillslope length, slope, storm duration and precipitation excess indicates the dramatic effect of the hydraulic resistance of the surface, and emphasizes the value of field measurements of this parameter on a variety of other surfaces. According to fig. 3, the range of K values used for the three hydrographs reflects differences in vegetation cover similar respectively to those of the sandy clay Luvisols (plots 6, 7, 10, 12,

13) at Kimana and Amboseli (K ~ 100), the Athi-Kapiti plots 3 and 5 after clipping to a basal cover of 36 % (K ~ 1000), and plots 3 and 5 with their original vegetation cover close to 77 % (K ~ 10,000). The lowest K value used is somewhat lower than those in figs. 3 b and 3 c, and probably represents the smoothest hillslope on the sandy clay without vegetation or a thin gravel cover. An extreme value is used here to demonstrate the full range of conditions in Kajiado District to the nearest order of magnitude.

Because the resistance is the variable with the largest range, it has a dominant effect on the storm duration required to obtain steady-state runoff (t_s is proportional to $K^{0.33}$, according to equation 8 a), and therefore on the peak runoff rate when steady state is not attained. On a densely vegetated hillside (K = 10,000 in fig. 7 b) discharge rises slowly and does not approach steady state before reaching a maximum that is less than one-sixteenth of that on the

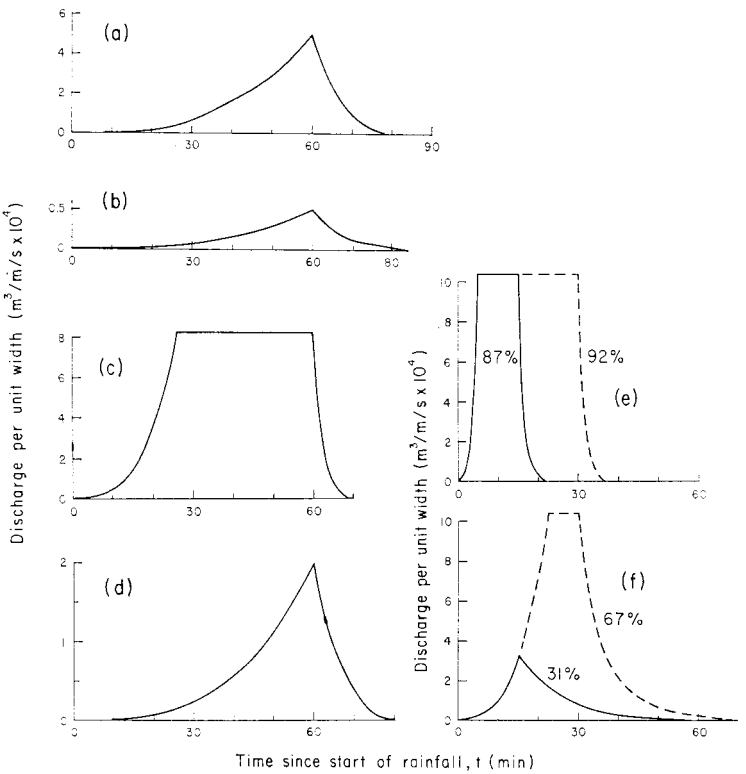

Fig. 7. Hydrographs of runoff under the following conditions: (a)–(d) are from one-hour rainstorms generating 10 mm/hr of precipitation excess on 300 m-long hillsides with an infiltration capacity of 25 mm/hr. (a) K = 1000, s = 0.025; (b) K = 10,000, s = 0.025; (c) K = 100, s = 0.05; (d) K = 10,000, s = 0.10. (e)–(f) are for 15-min (solid curves) and 30-min (dashed curves) rainstorms generating 75 mm/hr of precipitation excess on 50 m-long hillsides with gradients of 0.025 and infiltration capacities of 25 mm/hr under the following conditions: (e) K = 100, (f) K = 1000.

smoothest hillside (fig. 5) during the same rainstorm. Insertion of K = 10,000 into equation 8 a indicates that a storm duration of 2.6 hours would be necessary to bring hillside runoff to steady state if p = 10 mm/hr.

The resistance factor also affects the form of the recession limb and the total runoff since high flow resistance causes water to drain slowly from the hillside, allowing a relatively long time for infiltration. The runoff yield for the one-hour storm in fig. 7 a is less than 2 mm, and for that in fig. 7 b is only 0.2 mm. In these calculations, we have kept the infiltration capacity constant while varying the vegetation-dominated hydraulic resistance. Our experiments were not sufficiently numerous for recognition of possible effects of vegetation cover on infiltration. On other hillsides, the two variables may vary together, thereby enhancing the effects on runoff yield observed in our calculations.

Equation 8 a indicates that for a given hillslope length and rainfall intensity, the equilibration time for runoff is inversely proportional to the cube root of gradient. On the sandy clay Luvisols at Amboseli and Kimana, almost all gradients lie between 0.01 and 0.05, while on the Athi-Kapiti Plains the range is from 0.02 to 0.10. Figs. 7 c and 7 d illustrate hydrographs from the steepest of these gradients under conditions that are otherwise identical with those for figs. 5 and 7 b respectively. On the smoother slopes, steady state is attained 7 minutes earlier with the higher gradient, and the recession limb is slightly steeper. The total runoff was 0.5 mm (8 %) greater on the steeper slope. A more important difference results from the fourfold increase in gradient on the thickly vegetated Athi-Kapiti hillside (figs. 7 b and 7 d). The rising limb attained a peak discharge four times greater than that on the gentler gradient and the total runoff was almost four times greater on the steeper slope, although it still amounted to less than ten percent of the original precipitation excess.

The influence of surface resistance and hillslope length and gradient are affected by their interactions with the rate and duration of precipitation excess. The companion paper (DUNNE & DIETRICH, p. 50) lists the rainfall intensity-duration-frequency regime estimated for each of the measurement sites. Intensities (class mid-points) range up to about 100 mm/hr for 15- to 30-minute storms, and duration of the lower-intensity runoff-producing storms range up to about 4.5 hours. There are differences in the frequencies of each intensity-duration class between the three regions. It was also concluded that on the sandy clay Luvisols the infiltration capacity averages about 30 mm/hr at the beginning of the wet season and 25 mm/hr after the absorption of various amounts of rainfall (DUNNE & DIETRICH, this volume, fig. 5).

It is not possible to use the simple kinematic-wave procedure to compute hydrographs from our standard 300 m-long hillside with a precipitation excess of (say) 75 mm/hr because under these conditions the runoff becomes turbulent. This effect on the long Kenyan hillslopes will be considered in a later paper. In order to examine the effect of precipitation excess alone, we will compute hydrographs from a hypothetical 50 m-long hillside on which the Reynolds Number reaches only 1040 even with a runoff rate of 75 mm/hr. In figs. 7 e and 7 f we have compared hydrographs resulting from 75 mm/hr of precipitation excess for durations of 15 and 30 minutes on a bare soil for which K = 100 and a densely vegetated surface (K = 10,000). The gradient was 0.025, as in the

case of figs. 5, 7 a, and 7 b. The high rate of precipitation excess produces a more rapid rate of increase of runoff than in figs. 5 and 7 b, and the equilibration time is inversely proportional to the two-thirds power of the intensity of excess precipitation (eq. 8 a). Peak discharge and total runoff volume are particularly sensitive to the time required for the attainment of steady state, as indicated by figs. 7 c and 7 f. On the smoother hillside, 87 % and 92 % respectively of the precipitation excess on 15- and 30-minute rainstorms contributes to channel flow, whereas on the rougher hillside the values are 31 % and 67 % respectively. These proportions are much higher than corresponding totals of runoff in figs. 7 b and 7 d for a 300 m-long hillside with $p = 10$ mm/hr. The vast majority of runoff-producing storms in Kajiado District are of less than one-hour duration (DUNNE & DIETRICH, this volume), and therefore runoff does not usually reach equilibrium on most hillsides. Empirical formulae, frequently used to compute the time of concentration (Soil Conservation Service 1972) or the travel time of overland flow (RANTZ 1971), produce serious underestimation of the time required for the establishment of steady-state runoff on these savanna hillslopes.

Conclusion

With the aid of the kinematic-wave procedure based on field measurements of the hydraulic resistance properties of hillslope surfaces it is possible to compute average depths and velocities of Horton overland flow which are necessary for understanding geomorphic processes and for predicting soil erosion. We have described the nature of sheetflow and its local variability, and have provided evidence that a Moody diagram can be defined for natural hillslopes. Our calculations illustrate the effects on the runoff hydrograph of a realistic range of surface resistance, gradient, infiltration capacity and precipitation intensity for these savanna landscapes. The kinematic-wave procedure has been modified to allow infiltration after the rainstorm. This modification yields more realistic hydrographs and leads to some important insights about runoff from long, gentle hillslopes with high surface resistance. In particular, it becomes apparent that most of the precipitation excess generated on slopes with high hydraulic resistance never reaches the channel, but is responsible for a spatial variation in soil-moisture recharge and therefore plant production. The total annual runoff can only be computed when we develop hydrographs of runoff that begins as laminar flow and becomes turbulent on a long hillslope. However, it is already apparent that the runoff total is a small proportion of the precipitation excess derived in the companion paper. The method also allows the computation of partial-area contributions of Horton overland flow.

Acknowledgements

The field experiments were supported by Wildlife Management Project of FAO and the Kenya Ministry of Tourism and Wildlife. The assistance of M. J. BRUNENGO and D. WESTERN made the experiments possible. A. NOWELL helped us with the interpretation of the hydraulic data, and S. C. COLBECK and D. A. WOOLHISER advised us about the kinematic-wave procedure.

References

DUNNE, T., & W. E. DIETRICH (1980): Experimental study of Horton overland flow on tropical hillslopes: I. Soil conditions, infiltration and frequency of runoff. – (This volume).

EMMETT, W. W. (1970): The hydraulics of overland flow on hillslopes. – U.S. Geol. Survey Prof. Paper 662-A.

FOSTER, G. R., & L. D. MEYER (1975): Mathematical simulation of upland erosion by fundamental erosion mechanics. – In Present and prospective technology for predicting sediment yields and sources. U.S. Dept. Agric. Pub. ARS-S-40.

HENDERSON, F. M., & R. A. WOODING (1964): Overland flow and groundwater flow from a steady rainfall of finite duration. – J. Geophysic. Res., **69**: 1531–1540.

HORTON, R. E. (1945): Erosional development of streams and their drainage basins. – Geol. Soc. Amer. Bull., **56**: 275–370.

HORTON, R. E., H. R. LEACH, & R. VAN VLIET (1934): Laminar sheetflow. – Trans. Amer. Geophys. Union, **15**: 393–404.

IZZARD, C. F. (1944): The surface profile of overland flow. – Trans. Amer. Geophys. Union, **25**: 959–968.

KAO, D. T. Y., & B. J. BARFIELD (1978): Prediction of flow hydraulics for vegetated channels. – Amer. Soc. Agr. Eng. Trans., **21**: 489–494.

LANGFORD, K. J., & A. K. TURNER (1972): Effects of rain and depression storage on overland flow. – Civ. Eng. Trans., Inst. Civ. Engrs., Aust., **14**: 137–141.

MORGALI, J. R. (1970): Laminar and turbulent overland flow. – Proc. Amer. Soc. Civ. Engr., **96**: 441–460.

PARSONS, D. A. (1949): Depths of overland flow. – U.S. Dept. of Agric., Soil Conservation Service Tech. Pub. 82, 33 pp.

PHELPS, H. O. (1970): The friction coefficient for shallow flows over a simulated turf surface. – Water Resour. Res., **6**: 1220–1226.

RANTZ, S. E. (1971): Suggested criteria for hydrologic design of storm drainage facilities in the San Francisco Bay Region, California. – U.S. Geol. Survey Open File Report, Menlo Park, California.

REE, W. O. (1939): Some experiments on shallow flows over a grassed slope. – Amer. Geophys. Union Trans., **20**: 653–656.

SHERMAN, B., & V. P. SINGH (1976): A distributed converging overland flow model: II Effect of infiltration. – Water Resour. Res., **12**: 897–901.

SIMONS, D. B., & F. SENTÜRK (1978): Sediment transport technology. – Water Resources Pubs., Fort Collins, CO.

SINGH, V. P. (1976): A distributed converging overland flow model: III Application to natural watersheds. – Water Resour. Res., **12**: 902–908.

Soil Conservation Service (1972): Hydrology, Section 4, National Engineering Handbook, Washington, D.C.

WOOLHISER, D. A. (1975): Simulation of unsteady overland flow. – In K. MAHMOOD & V. M. YEVJEVICH (eds.): Unsteady Flow in Open Channels. – Water Resources Pubs., Fort Collins, CO: 485–508.

WOOLHISER, D. A., C. L. HANSON, & A. R. KUHLMAN (1970): Overland flow on rangeland watersheds. – J. Hydrol. (NZ), **9**: 336–356.

YOON, Y. N., & H. G. WENZEL (1971): Mechanics of sheetflow under simulated rainfall. – Proc. Amer. Soc. Civ. Engr., J. Hydr. Div., **97**: 1367–1386.

Address of the authors: T. DUNNE and W. E. DIETRICH, Department of Geological Sciences and Quaternary Research Center, University of Washington, Seattle, WA, 98105, U.S.A.